Gas-Phase Solvation of O_2^+, O_2^-, O_4^-, O_3^-, and CO_3^- with CO

Kenzo Hiraoka,* Jun Katsuragawa, Teruaki Sugiyama, Susumu Fujimaki, and Takanori Kojima

Clean Energy Research Center, Yamanashi University, Takeda-4, Kofu 400-8511, Japan

Shinichi Yamabe*

Department of Chemistry, Nara University of Education, Takabatake-cho, Nara 630-8528, Japan

Received: October 30, 2002; In Final Form: March 7, 2003

Equilibria for the gas-phase clustering reactions of O_2^+, O_2^-, O_4^-, O_3^-, and CO_3^- with CO were measured with a pulsed electron-beam mass spectrometer. Van't Hoff plots of the equilibrium constants led to the determination of the thermochemical stabilities for cluster ions. QCISD(T)/6-311(+)G(d,p)//UB3LYP/6-311+G(2d,p) calculations were performed to examine cluster geometries and interaction energies. The cluster ion $O_2^+(CO)_n$ was found to have the shell structure of $O_2^+(CO)_4(CO)_4(CO)_{n-8}$, whereas $O_4^-(CO)_n$ has the one of $O_4^-(CO)_4(CO)_2(CO)_4(CO)_{n-10}$. O_3^- and CO_3^- ions are solvated preferably by three and two CO ligands, respectively. The nucleophilicity of CO is larger than the electrophilicity. The characteristic nature of the bonding of the cluster ions of CO were compared with that of N_2.

1. Introduction

Precise measurement of the equilibrium constants for gas-phase ion/molecule clustering reactions at different temperatures leads to a determination of $\Delta H°$ and $\Delta S°$. Their accurate values give information on the nature of bonding in cluster ions. So far, not much work has been performed[1] that dealt with the inorganic gases. Cluster ions of these gases are generally weakly bound, and it is necessary to observe the equilibria of the clustering reactions at low temperatures, often below liquid N_2 temperature. In our laboratory, a determination of the inorganic gas cluster ions has been made by using a high-pressure mass spectrometer[2] that is equipped with a cryocooler. By use of this apparatus, it is possible to decrease the ion source temperature down to as low as 25 K. In the present study, clustering reaction 1 has been investigated,

$$A^{\pm}(CO)_{n-1} + CO = A^{\pm}(CO)_n \qquad (1)$$

where ions $A^{\pm} = O_2^+$, O_2^-, O_4^-, O_3^-, and CO_3^-. The main objective of the present study is to compare the solvating power of CO to that of N_2 and to obtain systematic information on the stabilities and structures of the positive and negative inorganic cluster ions.

The carbon monoxide has both nucleophilic and electrophilic centers on the carbon atom (Scheme 1). To positive ions, CO molecules are bound linearly. This coordination undergoes generally small steric crowding. In contrast, to negative ions, they are bound in the bent form. Generally, the coordination undergoes large steric crowding. In some cases, the cluster growth might be prohibited. The nitrogen molecule has smaller nucleophilicity and electrophilicity. This vague donor or acceptor property of N_2 would give cluster geometries different from those of CO. The fundamental coordination pattern of CO and N_2 molecules needs to be investigated by the use of small ions. If ions (A^+ and A^-) have complex structures, the pattern will be modified by the secondary interactions. This is a reason we adopted diatomic (O_2^+ and O_2^-), triatomic (O_3^-), and tetra-atomic (O_4^- and CO_3^-) ions. Negative ions were mainly examined to check the ligand−ligand steric crowd.

SCHEME 1: Frontier Orbitals of Carbon Monoxide and Fundamental Coordinations of CO Ligands.

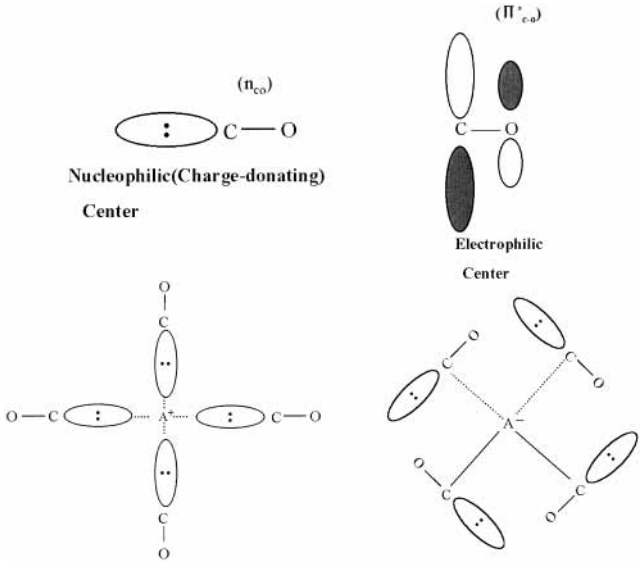

2. Experiments and Computations

The experiments were made with a pulsed electron-beam high-pressure mass spectrometer, which has been described previously.[2,3] The copper ion source equipped with a cryocooler (Iwatani Plantech, type-030) was used to perform low-temperature measurements. The major gas, CO or O_2, was passed through a dry ice−acetone-cooled molecular sieve trap (5 Å) and was fed into the ion source. The main chamber of the ion source was evacuated by a magnetic levitation turbomolecular pump (Seiko Seiki KK, STP-2000, 1950 L/s for N_2).

10.1021/jp022337o CCC: $25.00
Published on Web 05/23/2003

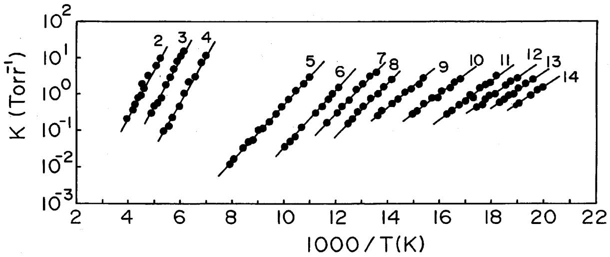

Figure 1. van't Hoff plots for clustering reaction $O_2^+(CO)_{n-1} + CO = O_2^+(CO)_n$.

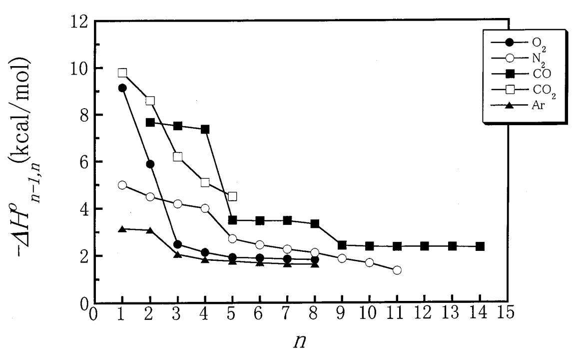

Figure 2. The *n* dependence of bond energies ($-\Delta H^\circ_{n-1,n}$) for the cluster ion $O_2^+(L)_n$, L = O_2,[7] N_2,[6] CO, CO_2,[8] and Ar.[9]

The reagent gas in the reaction chamber was ionized by a pulsed 2 keV electron beam. The ions produced were sampled through a slit made of razor blades (15 μm × 0.1 mm) and were mass analyzed by a quadrupole mass spectrometer (ULVAC, MSQ-400). To prevent charging, the inner surface of the ion source including an ion exit slit was coated with colloidal graphite.

Cluster systems are expected to be characterized by small molecular interaction energies. To describe them reliably, a large basis set needs to be employed. The 6-311+G(2d,p) basis set was used in the B3LYP[4] density functional theory calculations. The B3LYP/6-311+G(2d,p) geometry optimizations and the subsequent vibrational analyses were carried out to check whether the obtained geometry is correctly at a stable point and to obtain the zero-point vibrational energy (ZPE). Electronic energies were evaluated by a single-point QCISD(T)/6-311(+)G(d,p) calculation, where (+) means that the diffuse orbital is supplemented to 6-311G(d,p) for anionic systems. Theoretical binding energies (ΔEs) were obtained by the difference of ΔQCISD(T) and ΔZPE. All of the calculations were carried out by the use of Gaussian 98[5] program package installed on the Compaq ES40 computer at the Information Processing Center (Nara University of Education).

3. Results and Discussion

$O_2^+(CO)_n$ Clusters. When a mixed gas of 3.2 Torr of CO and 0.8 Torr of O_2 was ionized by 2 keV electrons, strong signals of O_2^+ and its cluster ions with CO molecules were observed. It was found that the $O_2^+(CO)_1$ ion decayed more slowly than O_2^+ in all of the temperature range measured and an equilibrium between O_2^+ and $O_2^+(CO)_1$ could not be established under the present experimental conditions. This is due to the unusually slow rate of the reaction $O_2^+ + CO \rightarrow O_2^+(CO)_1$. For reaction 1 with $n \geq 2$, equilibria could be readily observed down to the condensation point of the reagent gas CO (~50 K). The temperature dependence of the equilibrium constants is displayed in Figure 1 as van't Hoff plots. The obtained thermochemical data for $A^+ = O_2^+$ are summarized in Table 1, together with those for $O_2^+(N_2)_n$.[6]

TABLE 1: Experimental ($\Delta H^\circ_{n-1,n}$ and $\Delta S^\circ_{n-1,n}$) and Calculated (ΔE) Thermochemical Data for the Gas-Phase Clustering Reaction 1 for $A^\pm = O_2^+, O_2^-, O_3^-, O_4^-$, and CO_3^- [a,c]

	$O_2^+(CO)_n$		$O_2^+(N_2)_n$		$O_2^-(CO)_n$		$O_2^-(N_2)_n$		$O_3^-(CO)_n$		$O_3^-(N_2)_n$		$O_4^-(CO)_n$		$CO_3^-(CO)_n$	
n	$-\Delta H^\circ_{n-1,n}$	$-\Delta S^\circ_{n-1,n}$	$-\Delta H^\circ_{n-1,n}$	$-\Delta S^\circ_{n-1,n}$	$-\Delta H^\circ_{n-1,n}$	$-\Delta S^\circ_{n-1,n}$	$-\Delta H^\circ_{n-1,n}$	$-\Delta S^\circ_{n-1,n}$	$-\Delta H^\circ_{n-1,n}$	$-\Delta S^\circ_{n-1,n}$	$-\Delta H^\circ_{n-1,n}$	$-\Delta S^\circ_{n-1,n}$	$-\Delta H^\circ_{n-1,n}$	$-\Delta S^\circ_{n-1,n}$	$-\Delta H^\circ_{n-1,n}$	$-\Delta S^\circ_{n-1,n}$
1			5.0	17	3.5$_8$	18.$_9$					2.7$_2$	18.$_4$	3.4$_6$	15.$_2$	2.8$_2$	15.$_5$
	[8.6]		[5.74]		[3.64]		[3.08]		[3.86]		[2.75]					
2	7.6$_7$	21.$_0$	4.5	19	~3.4	(20)[b]			2.8$_9$	13.$_5$	2.6$_2$	19.$_6$	3.4$_4$	17.$_6$	2.7$_9$	16.$_4$
	[6.88]		[5.94]		[3.41]		[3.41]		[3.60]		[2.89]					
3	7.5$_2$	26.$_5$	4.2	19.$_6$					2.7$_1$	16.$_1$	2.5$_4$	19.$_7$	3.4$_1$	22.$_8$	2.4$_7$	15.$_2$
	[6.33]		[5.28]													
4	7.3$_7$	32.$_1$	4.0	22.$_5$					2.5$_4$	17.$_7$	2.2$_6$	20.$_2$	3.4$_0$	26.$_6$	2.3$_9$	16.$_3$
	[5.77]		[5.43]													
5	3.5$_0$	23.$_1$	2.7$_1$	16.$_2$					2.5$_2$	18.$_5$	2.0$_6$	18.$_7$	3.0$_7$	26.$_8$		
6	3.4$_7$	28.$_0$	2.4$_5$	16.$_1$					2.5$_1$	19.$_2$	1.9$_7$	19.$_0$	3.0$_5$	29.$_5$		
7	3.4$_7$	30.$_6$	2.2$_6$	18.$_5$							1.8$_2$	18.$_2$	2.5$_5$	26.$_5$		
8	3.3$_3$	31.$_7$	2.1$_1$	19.$_3$							1.7$_0$	17.$_5$	2.4$_9$	27.$_6$		
9	2.4$_2$	22.$_3$	1.8$_9$	19.$_1$							1.5$_1$	16.$_9$	2.3$_8$	28.$_0$		
10	2.3$_7$	24.$_6$	1.6$_8$	20.$_8$									2.2$_1$	28.$_0$		
11	2.3$_6$	27.$_7$	1.3$_5$	20.$_2$									1.7$_4$	23.$_4$		
12	2.3$_6$	29.$_2$														
13	2.3$_5$	30.$_7$														
14	2.3$_3$	32.$_4$														

[a] Data of $O_2^+(N_2)_n$ and $O_3^-(N_2)_n$ are taken from ref 6 and ref 10, respectively. $\Delta H^\circ_{n-1,n}$ and ΔE are in kcal/mol, and $\Delta S^\circ_{n-1,n}$ is in eu (standard state, 1 atm). Experimental errors for $\Delta H^\circ_{n-1,n}$ and $\Delta S^\circ_{n-1,n}$ are about ±0.3 kcal/mol and ±2 eu, respectively. Energies (ΔEs) in brackets are the computed ones. [b] Entropy value $-\Delta S^\circ_{1,2}$ is assumed to be 1 eu larger than that of $-\Delta S^\circ_{0,1}$ because of the loss of freedom of motion for ligands with growth of the cluster. [c] The subscript number in $\Delta H^\circ_{n-1,n}$ and $\Delta S^\circ_{n-1,n}$ means that the number is not necessarily reliable to this digit, but it indicates the subtle and meaningful difference among the measured values.

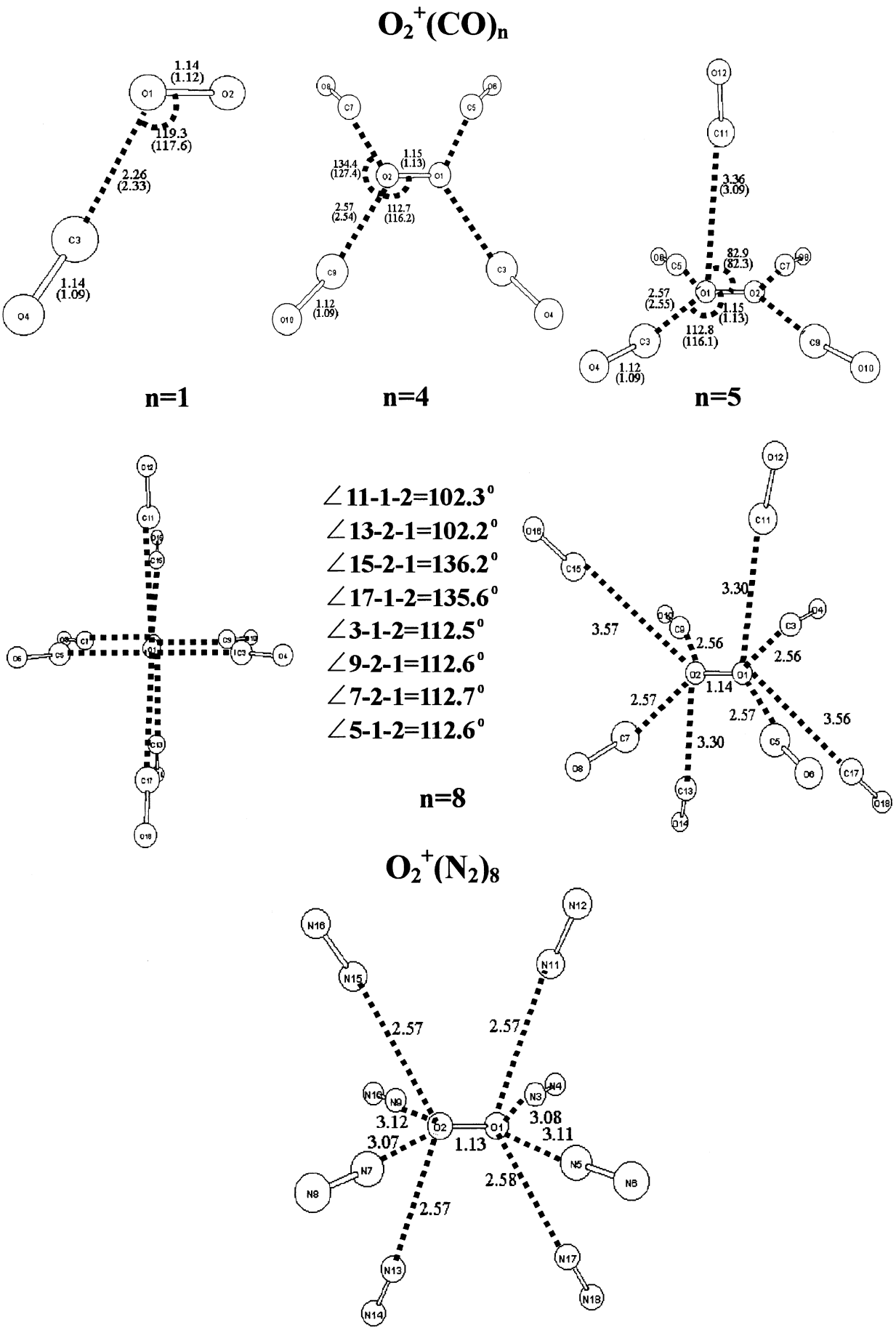

Figure 3. Geometries of $O_2^+(CO)_n$ clusters optimized by UB3LYP/6-311+G(2d,p). For $n = 1$, 4, and 5, distances in parentheses are for $O_2^+(N_2)_n$ also obtained in the present work. Geometries of $O_2^+(CO)_8$ and $O_2^+(N_2)_8$ are somewhat different and are shown separately.

SCHEME 2: Orbital Interactions Involved in $O_2^+(CO)_1$ and Its Radical Character

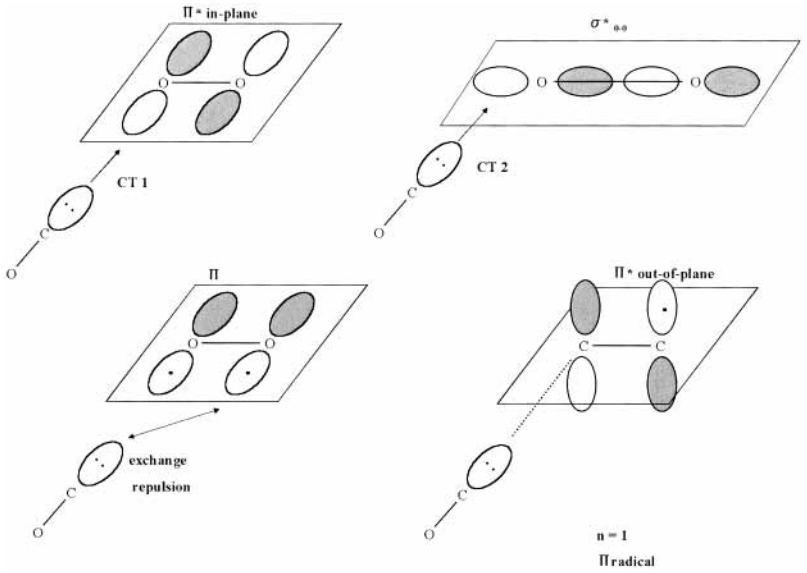

In the van't Hoff plots in Figure 1, there appear gaps between $n = 4-5$ and $8-9$. Figure 2 shows the n dependence of bond energies (i.e., $-\Delta H^\circ_{n-1,n}$) for cluster ions $O_2^+(L)_n$ with ligands L = CO, N_2,[6] O_2,[7] CO_2,[8] and Ar.[9] For L = CO, irregular decreases of $-\Delta H^\circ_{n-1,n}$ are observed between $n = 4-5$ and $8-9$. The values of $-\Delta S^\circ_{n-1,n}$ also show irregular decreases between $n = 4-5$ and $n = 8-9$ in Table 1. This sharp falloff strongly suggests that the cluster ion $O_2^+(CO)_n$ has the shell structure $O_2^+(CO)_4(CO)_4(CO)_{n-8}$. The distinct shell formation with $n = 4$ and 8 can be a clue for the elucidation of the structure of the cluster ion. The HOMO−LUMO interactions between the highly directional 5σ orbital of CO (HOMO) and the π^* orbitals of the core O_2^+ ion (LUMO) may explain the shell formation. The first four CO ligands would interact with the vacant π^* orbital and the second four CO ligands do with the singly occupied π^* orbital. That is, the first and the second four CO ligands belong to the planes that are orthogonal to each other. For the cluster of O_2^+ with N_2 (isoelectronic with CO), the first shell formation with $n = 4$ is also observed as in the case for L = CO. But their bond energies are much smaller than $O_2^+(CO)_n$ and the second shell formation with $n = 8$ is not seen (Table 1). This indicates that the nucleophilicity of N_2 is much weaker than that of CO.

It should be noted that the shell completion with $n = 2$ is observed for the cluster ions $O_2^+(O_2)_n$[7] and $O_2^+(CO_2)_n$.[8] It is evident that the positive charge is delocalized to some extent in the clusters with $n = 2$ for these cluster ions. For all of the clusters of O_2^+, O_4^+, and O_6^+ with Ar,[9] the shell formation with $n = 2$ was observed. Considering that the bond energies are on the order of a few kcal/mol, the nature of bonding in these clusters must be mainly electrostatic. The shell formation with $n = 2$ instead of $n = 4$ for $O_2^+(Ar)_n$ suggests that this cluster ion is bound by a nondirectional ion-induced dipole interaction rather than a directional HOMO−LUMO interaction.

Figure 3 shows geometries of $O_2^+(CO)_n$ ($n = 1$, 4, 5, and 8), along with those of $O_2^+(N_2)_n$. The $O_2^+(CO)_1$ geometry comes from two charge-transfer interactions, CT_1 and CT_2 in Scheme 2.

The exchange repulsion would be also a factor to determine the $n = 1$ geometry. However, the factor is small, because the ∠OC···O−O angle (119.3°) is similar to ∠N_2···O−O one (117.6°). If the factor were large, the ∠OC···O−O angle should be larger than the ∠N_2···O−O one because of the different extent of the repulsion. To undergo CT_1 and CT_2, an odd electron is in $\pi^*_{out-of-plane}$. The $O_2^+(CO)_1$ is a π radical, and four CO molecules may be in-plane coordinated equivalently. In fact, the $O_2^+(CO)_4$ has D_{2h} symmetry in Figure 3. The fifth and additional CO molecules are reinforced to be out-of-plane linked with $O_2^+(CO)_4$. An exchange repulsion between the radical spin density and the lone-pair electrons of CO cannot be avoided. A weak coordination in $O_2^+(CO)_5$ is seen in Figure 3. The $O_2^+(CO)_8$ geometry is shown as a second saturation shell. Noteworthy are somewhat different out-of-plane ($n > 5$) coordinations between $O_2^+(CO)_n$ and $O_2^+(N_2)_n$. While $O_2^+(N_2)_8$ has practically D_{2h} symmetry, $O_2^+(CO)_8$ has C_{2h} one.

SCHEME 3: A C_{2h}-Symmetry Geometry of $O_2^+(CO)_8$

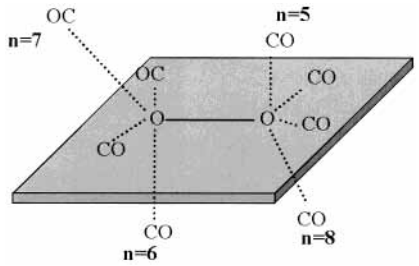

The fifth and sixth CO molecules persist in the perpendicular coordination along the $\pi^*_{out-of-plane}$. The seventh and eighth ones are coordinated nonorthogonally to the O−O bond (Scheme 3).

$O_2^-(CO)_n$. The observation of equilibria for the clustering reaction of O_2^- with CO was very tricky because of the rapid conversion of $O_2^-(CO)_1$ to $O_2^-(O_2)_1$ by reaction 2. Apparently,

$$O_2^-(CO)_1 + O_2 = O_2^-(O_2)_1 + CO \qquad (2)$$

reaction 2 is exothermic, that is, $O_2^-(O_2)_1$ is more stable than $O_2^-(CO)_1$. The cluster ions $O_2^-(CO)_n$ with $n \geq 3$ were too weak to observe the equilibria. Thermochemical data for the clustering reaction of O_2^- with L = CO is summarized in Table 1. For L = O_2[7] and CO_2,[10] a sudden decrease in $-\Delta H^\circ_{n-1,n}$ between $n = 1$ and 2 was observed. This is due to the negative charge dispersal in the complexes $O_2^-(O_2)_1$[7] and $O_2^-(CO_2)_1$.[10] Instead, the interaction of O_2^- with CO in Table 1 is only electrostatic. It is apparent that the electrophilicity of the CO molecule is much smaller than that of O_2 and CO_2 ligands.

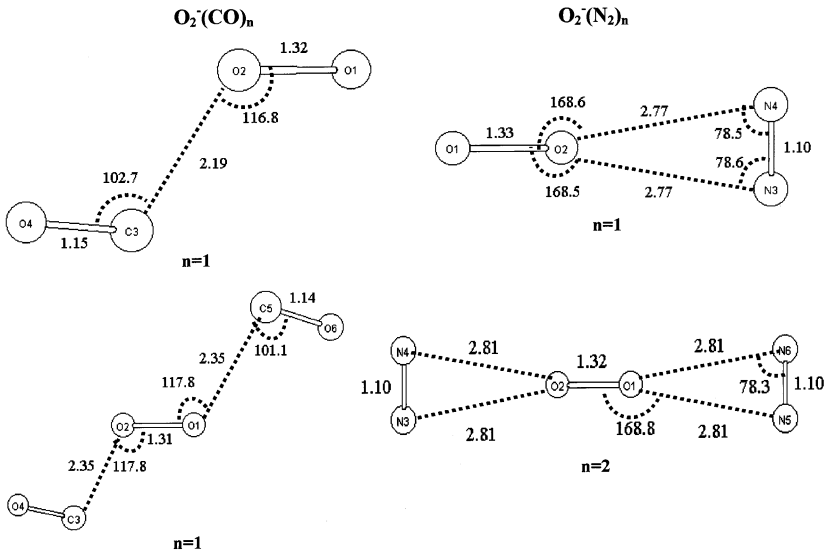

Figure 4. Geometries of $O_2^-(CO)_n$ and $O_2^-(N_2)_n$ clusters.

SCHEME 4: The Charge-Transfer Attraction and Exchange Repulsion Involved in $O_2^-(CO)_1$

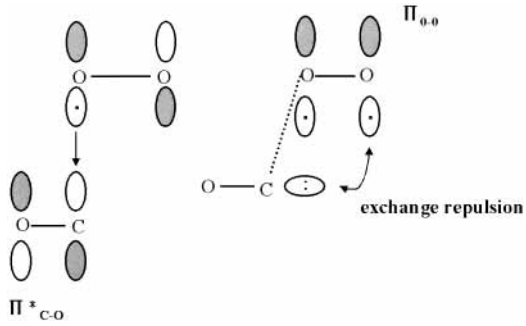

In Table 1, the bond energies of $O_2^+(CO)_n$ with $n = 1-4$ (>7 kcal/mol) are much larger than that of $O_2^-(CO)_1$ (3.58 kcal/mol). It is evident that the nucleophilicity (basicity) of CO is greater than the electrophilicity (acidity). In the nucleophilic attack, the highly directional 5σ HOMO of CO plays a major role and a charge transfer in the complex takes place to some extent. In the electrophilic attack, the HOMO of CO must experience a considerable exchange repulsion against the electron cloud of the negative ion, resulting in the mainly electrostatic interaction.

Figure 4 exhibits geometries of $O_2^-(CO)_n$, $n = 1$ and 2, along with those of $O_2^-(N_2)_n$. $O_2^-(CO)_1$ is a σ radical. The large $\angle$OC$\cdot\cdot$O$-$O angle, 116.8°, comes from the exchange repulsion between π_{O-O} and the CO lone-pair (5σ HOMO), which is shown in Scheme 4. The $O_2^-(CO)_2$ cluster is of a symmetric (C_{2h}) geometry. The $n \geq 3$ cluster geometries could not be obtained despite many trial initial geometries. Two lone-pair orbitals (5σ HOMO) preclude further CO coordinations. Thus, absence of $n \geq 3$ thermochemical data in Table 1 comes not from a technical problem in measurements but from the exclusive coordination of two CO molecules (Scheme 5). The $O_2^-(N_2)_1$ and $O_2^-(N_2)_2$ geometries are of C_{2v} and D_{2h} point groups, respectively. They are controlled by antisymmetric CT interactions in σ radicals (Scheme 6). As in $O_2^-(CO)_n$, $O_2^-(N_2)_n$ ($n > 2$) clusters could not be obtained.

In the interaction of O_2^- with CO ligands, the frontier orbitals of O_2^- direct the solvation morphologies. This trend was also observed earlier in the hydration of the O_2^- system.[11]

$O_3^-(CO)_n$. To increase the ion intensity of O_3^- ion, the O_2 gas was used as a major gas (3 Torr) and about 0.4 Torr of CO

SCHEME 5: The Exclusive Coordination of Two CO Molecules to O_2^-

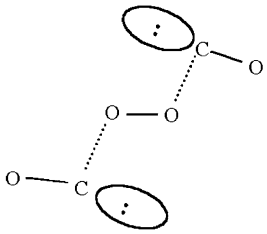

SCHEME 6: An Antisymmetric Charge-Transfer Interaction Determining the C_{2v} symmetry of $O_2^-(N_2)_1$

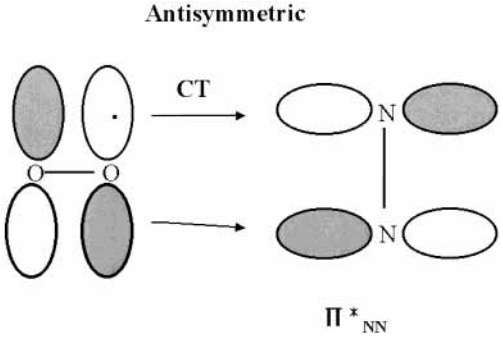

was introduced into the major O_2 gas through a stainless steel capillary. It was found that the equilibrium between O_3^- and $O_3^-(CO)_1$ could not be observed because of the slower decay of the latter ion than the former. This may be due to the contamination of the $O_3^-(CO)_1$ ion with the $O_2^-(CO_2)_1$. The impurity of CO_2 may be formed by reaction 3,

$$O^- + CO = CO_2 + e^- \qquad (3)$$

or by the complex radical reactions induced by the electron impact on the CO-containing reagent gas. With decrease of temperature lower than 170 K, a strong growth of $O_2^-(CO_2)_n$ with $n = 2-4$ with $m/z = 120$, 166, and 208, respectively, was observed, and the ratio of the ion intensities $I[O_3^-(CO)_2]/I[O_3^-(CO)_1]$ became time-independent after the electron pulse. This suggests that almost all of the $O_2^-(CO_2)_1$ was converted to the higher-order clusters $O_2^-(CO_2)_n$ with $n \geq 2$. The equilibrium constants for the reaction with $n \geq 2$ were found

(a) $O_3^-(CO)_n$

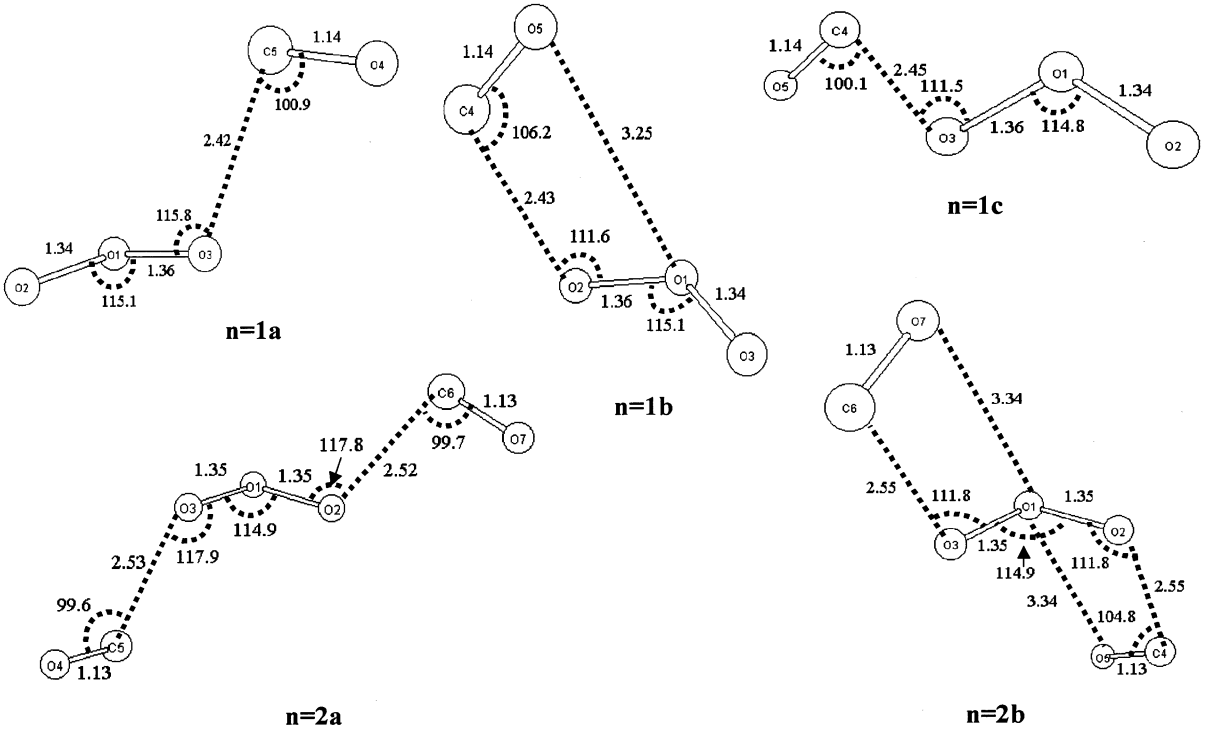

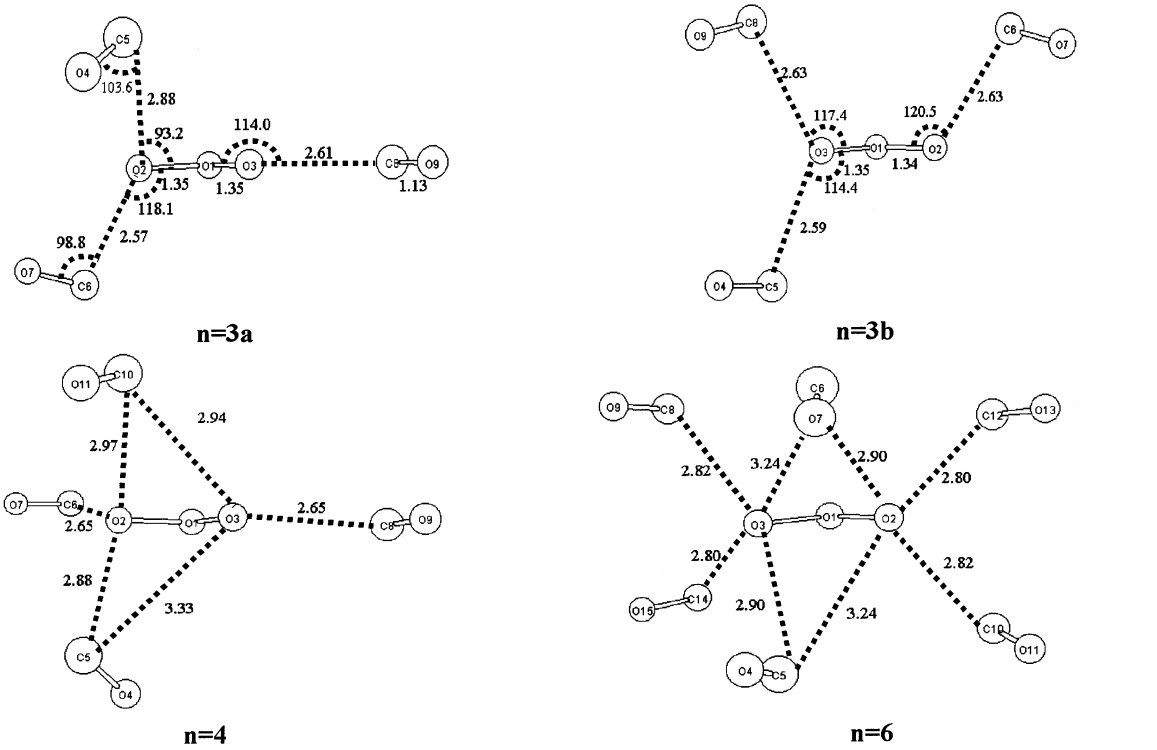

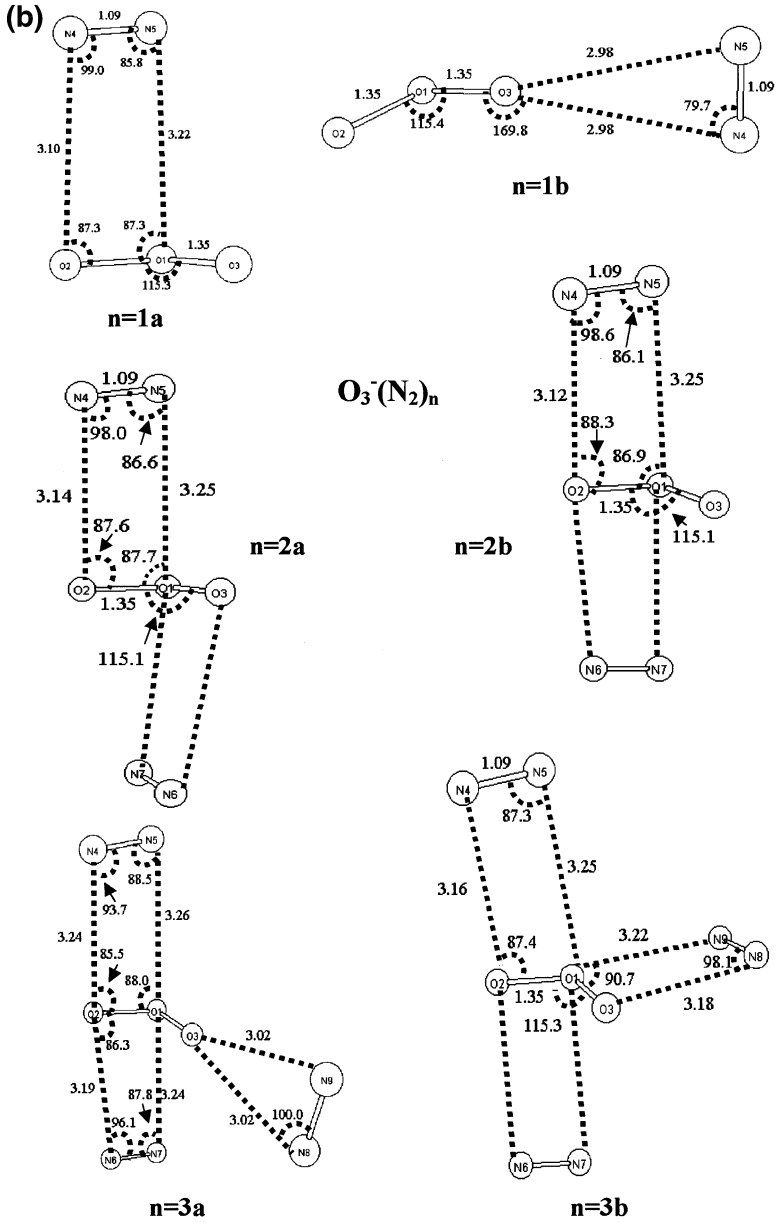

Figure 5. Geometries of (a) $O_3^-(CO)_n$ and (b) $O_3^-(N_2)_n$. Stability rank in geometric isomers is a > b > c (model a is most stable). In panel a, CO is linked with CO_3^- in its out-of-plane direction in $n = 1$a, while the $n = 1$c is of a planar geometry.

to be independent of the CO gas pressure below 170 K, that is, the establishment of equilibria for reaction 1 for $A^- = O_3^-$ with $n \geq 2$. The thermochemical data obtained from the van't Hoff plots are summarized in Table 1. An irregular decrease in $-\Delta H°_{n-1,n}$ was observed between $n = 3$ and 4, and the $-\Delta H°_{n-1,n}$ values become nearly *n*-independent with $n \geq 4$. It is a general trend that the core ion O_3^- is solvated preferentially by the first three ligand molecules as observed in $O_3^-(N_2)_n$ and $O_3^-(O_2)_n$. The solvating power is in the order of CO > N_2 > O_2 in $O_3^-(L)_n$. This may be reasonable because both the polarizabilities and quadrupole moments for these molecules are in that order.

Figure 5a shows geometries of $O_3^-(CO)_n$, $n = 1-4$, and 6. Three isomers of $O_3^-(CO)_1$ were found, the $n = 1$a model is most stable (Scheme 7). Although the two-center CT interaction in $n = 1$b is stronger than the one-center one in $n = 1$a, the former is counterbalanced by the exchange repulsion. The $O_3^-(CO)_2$ has an expected trans coordination shape. For $n = 3$, interestingly, $n = 3$a is more favorable than $n = 3$b. The $n = 3$b has a repulsion between two lone-pair electrons (Scheme 8). In $n = 4$, the repulsion reinforces the midway coordination of two CO molecules (C5O4 and C10O11), where the coordination of C6O7 and C8O9 is in the plane defined by the O_3^- ion (Scheme 9). The switch of the coordination pattern in $n = 3 \rightarrow 4$ leads to the falloff of bonding energies (2.71 → 2.54 kcal/mol) in Table 1. The $n = 6$ is a saturation model, and $n > 7$ coordinations are much less favorable. Figure 5b presents geometries of $O_3^-(N_2)_n$. A one-center out-of-plane coordination model of $O_3^-(N_2)_1$ was not found because the electrophilic center is not localized in one nitrogen atom (Scheme 10). The $O_3^-(N_2)_2$ geometry has two out-of-plane N_2 ligands. In $n = 3$a, exchange repulsions among N_2 ligands are avoided. Noteworthy are asymmetric $n = 3$a geometries of $O_3^-(CO)_3$ and $O_3^-(N_2)_3$. Both of them have sources of steric crowd for further ($n > 4$) ligand coordinations.

$O_4^-(CO)_n$. Equilibria for clustering reaction 1 for $A^- = O_4^-$ could be observed down to the temperature just above the condensation point of the major CO gas by introducing a small amount of O_2 into the CO major gas. The temperature dependence of the equilibrium constants is displayed as van't

SCHEME 7: SOMO → π^*_{CO} and (HOMO − 1) → π^*_{CO} Charge-Transfer Interactions in $O_3^-(CO)_1$

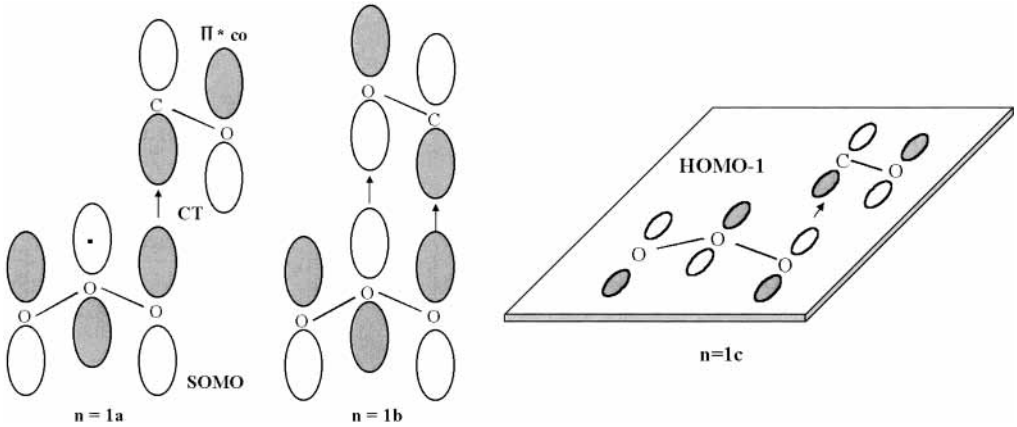

SCHEME 8: Exchange Repulsion between Two Out-of-Plane CO Ligands

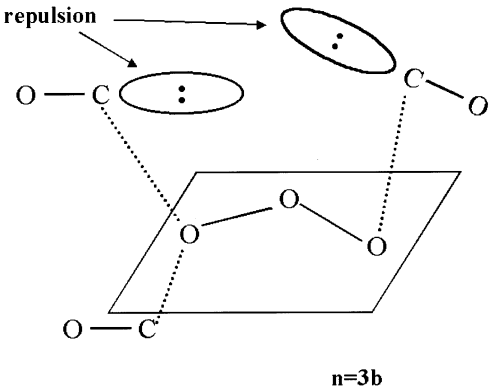

SCHEME 9: Dual Antisymmetric (HOMO→π^*_{CO}) Charge-Transfer Interactions in $O_3^-(CO)_4$

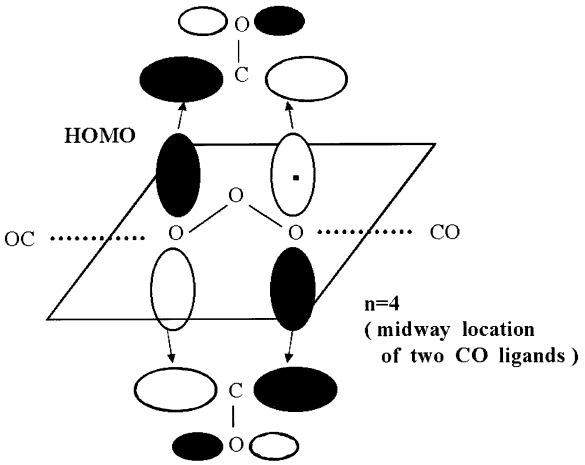

SCHEME 10: A One-Center Addition Model, Absent

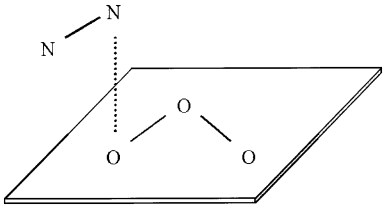

Hoff plots in Figure 6. Thermochemical data are summarized in Table 1. In Figure 6, there appear gaps between $n = 4-5$, 6−7, and 10−11. It seems likely that the cluster ion $O_4^-(CO)_n$ can be represented as a shell structure of $O_4^-(CO)_4(CO)_2$-

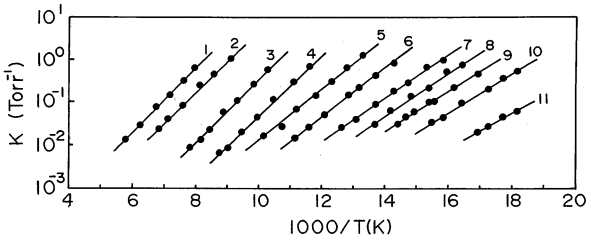

Figure 6. van't Hoff plots for clustering reaction $O_4^-(CO)_{n-1} + CO = O_4^-(CO)_n$.

$(CO)_4(CO)_{n-10}$. Such a distinct formation of high-order shell structure is unique, and it is tempting to conjecture the geometrical structure of the cluster ion. Thompson and Jacox investigated the vibrational spectra of O_4^- in solid neon.[12] They concluded that O_4^- possesses two equivalent O_2 units with a planar trans C_{2h} configuration. It may be conceivable that two each CO ligands may be accommodated by the terminal O atoms. The 5th and 6th CO may be accommodated by the central two O atoms. The 7th to 10th CO ligands may interact with the terminal O atoms such as the first CO ligands but in the plane orthogonal to that for the first four ligands.

$CO_3^-(CO)_n$. In this measurement, ∼0.4 Torr of CO and 70 mTorr of CO_2 were fed into the 3 Torr of O_2 major gas through stainless steel capillaries. The core ion CO_3^- may be produced by reactions 4 and 5.

$$O^- + CO_2 = CO_3^- \quad (4)$$

$$O_3^- + CO_2 = CO_3^- + O_2 \quad (5)$$

Thermochemical data obtained from the van't Hoff plots are summarized in Table 1. There is a small irregular decrease in $-\Delta H^\circ_{n-1,n}$ between $n = 2$ and 3. In our previous work,[15] it was pointed out that CO_3^- may be regarded as a carboxylic ion with a carbonyl bond. The preferable solvation of the first two CO ligands by CO_3^- may be due to the interaction of these CO molecules with two carboxylic O atoms in CO_3^-.

4. Concluding Remarks

In this work, gas-phase clusters, $O_2^+(CO)_n$, $O_2^-(CO)_n$, $O_3^-(CO)_n$, $O_4^-(CO)_n$, and $CO_3^-(CO)_n$, have been studied by the use of a pulsed electron-beam high-pressure mass spectrometry. For $O_2^+(CO)_n$, $O_2^-(CO)_n$, and $O_3^-(CO)_n$, cluster geometries have been examined by calculations in comparison with those of $O_2^+(N_2)_n$, $O_2^-(N_2)_n$, and $O_3^-(N_2)_n$. Except $O_2^+(CO)_n$ ($n = 1-4$), all species have given a few kcal/mol

bonding energies. These values have been satisfactorily reproduced by QCISD(T)/6-311(+)G(d,p)//UB3LYP/6-311+G(2d,p) ZPE energies in Table 1. Despite small binding energies, cluster geometries have been found to be frontier-orbital-controlled. In addition, the exchange repulsion by the lone-pair electrons (5σ HOMO) of CO influences them. In the extreme case, the third and higher clustering reactions in $O_2^-(CO)_n$ are prohibited by the repulsion.

References and Notes

(1) Keesee, R. G.; Castleman, A. W., Jr. *J. Phys. Chem. Ref. Data* **1984**, *15*, 1011.

(2) Hiraoka, K.; Yamabe, S. In *Dynamics of Excited Molecules*; Kuchitsu, K., Ed.; Elsevier: Amsterdam, 1994; p 399.

(3) Kebarle, P. In *Techniques for the Study of Ion−Molecule Reactions*; Farrar, J. M., Saunders, W. H., Jr., Eds.; Wiley: New York, 1988, p 221.

(4) Becke, A. D. *J. Chem. Phys.* **1993**, *98*, 5648.

(5) Frisch, M. J.; Trucks, G. W.; Schlegel, H. B.; Scuseria, G. E.; Robb, M. A.; Cheeseman, J. R.; Zakrzewski, V. G.; Montgomery, J. A., Jr.; Stratmann, R. E.; Burant, J. C.; Dapprich, S.; Millam, J. M.; Daniels, A. D.; Kudin, K. N.; Strain, M. C.; Farkas, O.; Tomasi, J.; Barone, V.; Cossi, M.; Cammi, R.; Mennucci, B.; Pomelli, C.; Adamo, C.; Clifford, S.; Ochterski, J.; Petersson, G. A.; Ayala, P. Y.; Cui, Q.; Morokuma, K.; Malick, D. K.; Rabuck, A. D.; Raghavachari, K.; Foresman, J. B.; Cioslowski, J.; Ortiz, J. V.; Stefanov, B. B.; Liu, G.; Liashenko, A.; Piskorz, P.; Komaromi, I.; Gomperts, R.; Martin, R. L.; Fox, D. J.; Keith, T.; Al-Laham, M. A.; Peng, C. Y.; Nanayakkara, A.; Gonzalez, C.; Challacombe, M.; Gill, P. M. W.; Johnson, B. G.; Chen, W.; Wong, M. W.; Andres, J. L.; Head-Gordon, M.; Replogle, E. S.; Pople, J. A. *Gaussian 98*, revision A.7; Gaussian, Inc.: Pittsburgh, PA, 1998.

(6) Hiraoka, K.; Nakajima, G. *J. Chem. Phys*. **1988**, *88*, 7709.

(7) Hiraoka, K. *J. Chem. Phys.* **1988**, *89*, 3190.

(8) Hiraoka, K.; Nakajima, G.; Shoda, S. *Chem. Phys. Lett*. **1988**, *146*, 535.

(9) Hiraoka, K.; Kudaka, I.; Yamabe, S. *J. Mass. Spectrom. Soc. Jpn*. **1995**, *43*, 65.

(10) Hiraoka, K. *Chem. Phys.* **1988**, *125*, 439.

(11) Weber, J. M.; Kelley, J. A.; Nielsen, S. B.; Ayotte, P.; Johnson, M. A. *Science* **2000**, *287*, 2461.

(12) Thompson, W. E.; Jacox, M. E. *J. Chem. Phys*. **1989**, *91*, 3826.

(13) Aquino, A. J. A.; Taylor, P. R.; Walch, S. P. *J. Chem. Phys.* **2001**, *114*, 3010.

(14) Kelley, J. A.; Robertson, W. H.; Johnson, M. A. *Chem. Phys. Lett.* **2002**, *362*, 255.

(15) Hiraoka, K.; Yamabe, S. *J. Chem. Phys.* **1992**, *97*, 643.